Molecular Basis for the Anisotropic Transverse Thermal Expansion of Syndiotactic Polypropylene

Daniel J. Lacks*

Department of Chemical Engineering, Tulane University, New Orleans, Louisiana 70118

Gregory C. Rutledge

Department of Chemical Engineering, Massachusetts Institute of Technology, Cambridge, Massachusetts 02139

Received April 24, 1995; Revised Manuscript Received June 2, 1995[⊗]

ABSTRACT: The thermal expansion of crystalline syndiotactic polypropylene is simulated to elucidate the origins of the transverse thermal expansion anisotropy observed in these materials. The calculations are carried out using a lattice dynamics method and empirical force fields. For the transverse thermal expansion coefficients, the results obtained for different crystal structures and force fields bracket the experimental results. Thermal expansion is calculated to be greater along the *b* axis than along the *a* axis, in agreement with experiment. This transverse thermal expansion anisotropy is found to arise from larger thermal stresses, lower stiffness, and less Poisson coupling along the *b* axis.

Introduction

Recent studies of the morphology of semicrystalline syndiotactic polypropylene (sPP) by Lovinger *et al.* have shown that cracks and ripples are common features in the crystallites.[1] These features are expected to severely degrade the mechanical properties of semicrystalline sPP and limit its end use. Since the cracks and ripples were found under all of the crystallization conditions studied and occurred periodically along the crystallite, it was suggested that they arise in response to a buildup of stresses which are inherent to the polymer material. It was proposed that these stresses develop upon the cooling of the material subsequent to crystallization, due to a mismatch of the thermal expansion coefficients in the crystallite and the chain-fold regions at the top and bottom of the lamella. In the crystalline regions, it was shown by X-ray diffraction that the thermal expansion transverse to the chain axis is highly anisotropic, being almost 1 order of magnitude larger along the *b* direction than along the *a* direction. The thermal expansion within the chain-fold regions is also expected to be highly anisotropic, with the thermal expansion being larger between the fold planes than within the fold planes. For sectors in which the anisotropies of the crystalline and chain-fold regions coincide, the thermal contraction with cooling proceeds normally; however, for sectors in which the anisotropies do not coincide, stresses develop upon cooling which lead to the observed ripples and cracks.

The present paper examines the molecular origins of the transverse thermal expansion anisotropy in the crystalline regions of sPP in order to elucidate the origins of the observed cracks and ripples. Simulations of the temperature dependence of sPP crystals are carried out that treat thermal expansion and elasticity from first principles. These simulations are similar to those in our previous studies of the thermophysical properties of crystalline polyethylene,[2] isotactic polypropylene,[3,4] and the aromatic polyamides poly(*p*-phenylene teraphthalamide) and poly(*p*-benzamide).[5]

[⊗] Abstract published in *Advance ACS Abstracts,* July 15, 1995.

Computational Method

The free energy of the crystal is calculated within the quasi-harmonic approximation with the interatomic potential energy surface parameterized by an empirical force field. The complete three-dimensional crystal structure is considered, and Ewald methods are used to evaluate the Coulombic and dispersion energy sums. Equilibrium unit cell volumes are obtained by minimizing the free energy at the specified temperature. Elastic stiffness moduli and Gruneisen parameters are calculated from the appropriate numerical derivatives of the free energy or entropy with strain, and the elastic compliance moduli are obtained by inverting the stiffness matrix. A detailed description of this computational method is given elsewhere.[2]

a. Free Energy Calculation. The vibrational free energy is evaluated within the quasi-harmonic approximation,[6] which neglects terms higher than second order in the Taylor expansion of the potential energy. The resulting harmonic potential energy surface and vibrational frequencies vary with the lattice parameters, thereby incorporating anharmonic effects due to volume changes but neglecting anharmonic coupling of the vibrational modes. Quantum mechanical effects, which are important for vibrational motion with frequencies $\nu > kT/h$ ($\sim$200 cm^{-1} at room temperature), are included. An analysis of the accuracy of the quasi-harmonic approximation and perturbative corrections is given elsewhere.[7]

The procedure used to obtain the free energy for a given set of lattice parameters begins with the minimization of the potential energy with respect to the variables describing the atomic positions within the unit cell. The vibrational frequencies and their contributions to the quantum mechanical free energy are then calculated at points throughout the Brillouin zone, and the total vibrational free energy is obtained by numerically integrating these contributions over the Brillouin zone. The equilibrium lattice parameters are those that minimize the total free energy, which is the sum of the potential energy and the vibrational free energy.

b. Force Fields. The calculations are carried out with two force fields, in order to elucidate the dependence of the results on the approximate nature of the force field. Modifications of the empirical force fields

0024-9297/95/2228-5789$09.00/0

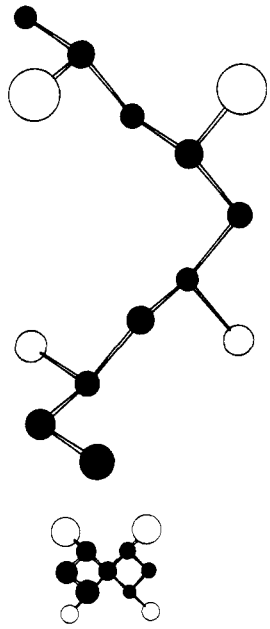

Figure 1. The s(2/1)2 configuration of the sPP chain. The size of the atom corresponds to its position in the direction perpendicular to the page. Hydrogen atoms are omitted for clarity. The top figure corresponds to the projection onto the $a-c$ plane of the crystal, and the bottom figure corresponds to the projection onto the $a-b$ plane.

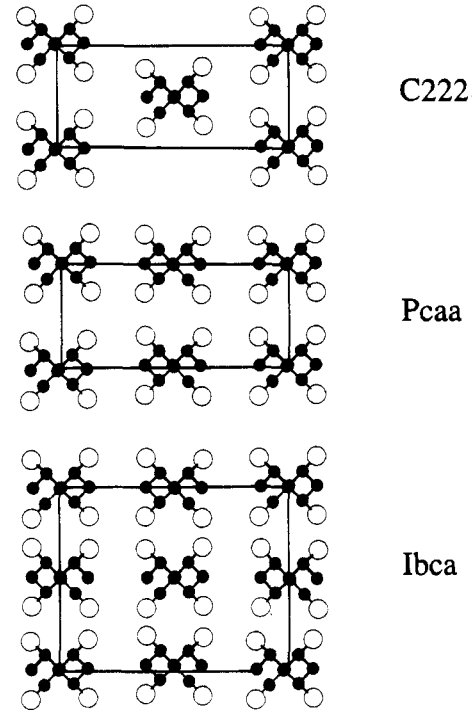

Figure 2. Proposed crystal structures of sPP. Hydrogen atoms are omitted for clarity. The a axes are horizontal, the b axes are vertical, and the c axes come out of the page.

of Sorensen *et al.*[8] (SLKB) and Karasawa *et al.*[9] (KDG), which we designate SLKB* and KDG*, were used. The KDG* force field has been modified to include CCC–CCC and CCC–CCH bend interactions required for proper representation of methyl group interactions. In the SLKB* force field, nonbonded interactions have been reparameterized to an exp–6 form with geometric mean mixing rules used for determining dispersion constants, which allow more efficient Ewald sum methods to be used. These modifications are described in more detail elsewhere.[4]

c. Crystal Structures. The minimum energy configuration for the sPP chain, shown in Figure 1, is a s(2/1)2 helix and is formed when the backbone torsion angles repeat the sequence trans–trans–gauche–gauche.[10] This helical structure is lower in energy under normal conditions than the all-trans structure because the intramolecular steric interactions between the methyl side groups are reduced (at high tensile stresses, however, the all-trans structure becomes more stable[11]).

The crystal structures that have been proposed for sPP are shown in Figure 2. The differences in these structures, which are all formed from s(2/1)2 helices, arise from differences in the chirality of the component chains. In the $C222_1$ structure, which was originally proposed for sPP,[12] all helices are of the same chirality. For *Pcaa*, the helices along the a axis alternate in chirality, while for *Ibca*, the helices alternate in chirality along both the a and b axes. The most recent experiments have shown that the crystal structure belongs to the space group *Ibca*,[13] but the $C222_1$ and *Pcaa* structures are thought to be present in small amounts as defect structures.[14–16]

The experimental $C222_1$, *Pcaa*, and *Ibca* structures are taken as the starting points for the calculations, but the atoms are allowed to relax to their minimum energy positions. The fully variable triclinic lattice, with 6 degrees of freedom, is used in the calculations. All chains in the unit cell are considered to be equivalent, and thus the variables describing the atomic positions within the unit cell consist of the coordinates of the atoms in the first chain and the setting angle and three translational offset coordinates for all other chains.

Results and Discussion

Calculations were carried out for sPP with both the SLKB* and KDG* force fields for the three crystal structures proposed for sPP. The energy-minimized structures that were obtained differ slightly from the structures determined from experiment. Most notably, the calculated structures corresponding to the *Pcaa* and *Ibca* structures included axial displacements of the chains: the calculated structure corresponding to *Pcaa* has the two chains within the unit cell displaced axially with respect to each other by 0.7 Å, and the calculated structure corresponding to *Ibca* has a monoclinic unit cell with the angle $\beta = 107°$. These differences from the experimentally determined structures may be due either to inaccuracies in the force fields or to the limited resolution of the experiments, which may have precluded the determination of such details (it is noted that the experimental data have shown some evidence of axial displacements, but these data were interpreted as arising from defects rather than the regular crystal structure[16]). No analysis is made of the relative stabilities of the crystal structures because the errors in the approximate force fields are most likely larger than the energy differences between the structures.

The calculated transverse thermal expansion coefficients for sPP are shown in Figure 3. There is a significant force field dependence of the thermal expansion coefficients, which obscure any distinction between the results for the different crystal structures—the results for the three crystal structures and the two force fields are therefore considered together, to give effective error bars for the calculation (it is noted that thermal expansion, which is the *change* in lattice parameters with temperature, is a sensitive property and uncer-

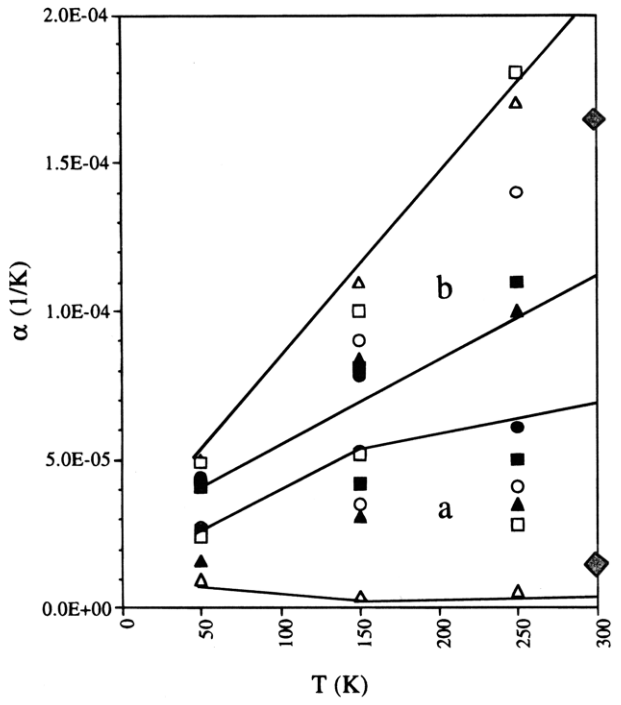

Figure 3. Transverse thermal expansion coefficients for sPP: squares, *Ibca* structure; circles, *Pcaa* structure; and triangles, $C222_1$ structure. Open symbols are for the SLKB* force field, and closed symbols are for the KDG* force field. The grey diamonds are the experimental results of Lovinger *et al.*[1] The lines are guides to the eye, which bracket the calculated results. The lower set of results is for the thermal expansion along *a*, and the upper set of results is for the thermal expansion along *b*.

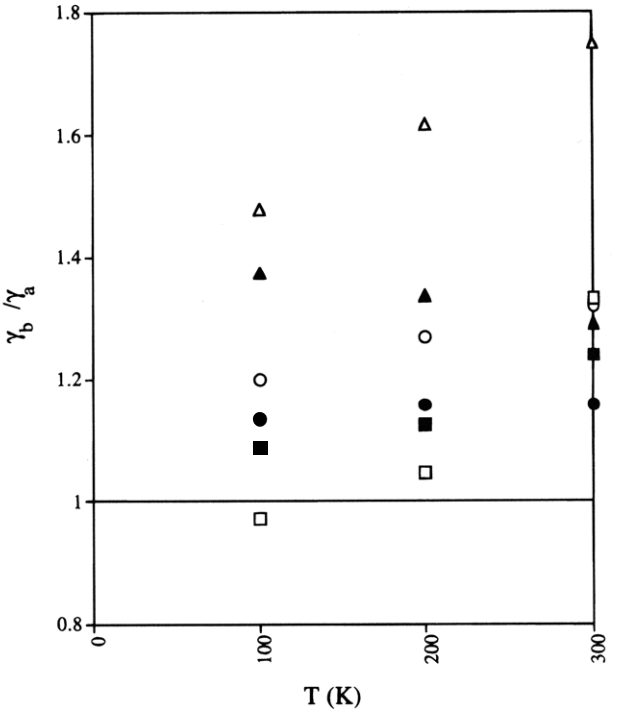

Figure 4. Ratio of the transverse Gruneisen parameters for sPP. Symbols are the same as in Figure 3.

tainties in the results must be expected; also, the loose helical structure of sPP makes the results particularly sensitive to the details of the forces fields, as compared to the other polymer crystals we have studied[2-5]). It is clear, however, that the calculations show α_b to be larger than α_a. The experimental results of Lovinger *et al.* for α_b and α_a at room temperature fall within the range of the calculated results. However, since most of the calculated values for α_a are larger than the experimental value, the thermal expansion anisotropy α_b/α_a is underestimated in comparison with experiment.

The factors influencing the magnitude of the thermal expansion coefficients are elucidated with the Gruneisen equation,

$$\alpha_i = (C_v/V)\sum_{j=1}^{6}\gamma_j S^T_{ij} \quad (1)$$

where V is the volume, C_v is the heat capacity at constant volume, S^T_{ij} is the isothermal compliance modulus, and i and j index the six strain components (in Voigt notation). In analogy with the stress–strain relations, α_i is a strain along i per degree of temperature, and $(C_v/V)\gamma_j$ is the thermal stress along j per degree of temperature. The Gruneisen parameter, γ_i, which represents the thermal stress per unit of thermal energy, is defined by

$$\gamma_i = (1/C_v)(\partial S/\partial \epsilon_i) \quad (2)$$

where S is the entropy and ϵ_i is the i component of strain. Thermal expansion along a given axis therefore arises from the elastic response to the thermal stress along that axis, plus the elastic response to the thermal stresses along the other axes (Poisson coupling). It is noted that the off-diagonal compliance moduli are usually negative and significantly smaller in magnitude than the diagonal compliance moduli.

In order to understand the molecular origins of the observed thermal expansion anisotropy in sPP, the differences in the Gruneisen parameters and the compliance moduli along the two transverse directions are examined. The results for the ratios of the Gruneisen parameters along these directions, given in Figure 4, show that the thermal stresses are larger along the *b* axis than along the *a* axis. The consequences of $\gamma_b > \gamma_a$ on the relevant terms in the Gruneisen equation,

$$\alpha_a = (C_v/V)[\gamma_a S^T_{aa} + \gamma_b S^T_{ab} + \gamma_c S^T_{ac} + ...] \quad (3a)$$

$$\alpha_b = (C_v/V)[\gamma_b S^T_{bb} + \gamma_a S^T_{ab} + \gamma_c S^T_{bc} + ...] \quad (3b)$$

are to increase α_b relative to α_a both by making the diagonal term larger along the *b* axis and by making the off-diagonal *a*–*b* coupling term larger *in magnitude* along the *a* axis (this off-diagonal term is negative).

The ratios of the diagonal compliance moduli along the transverse directions are shown in Figure 5. These compliance moduli are larger along the *b* axis than along the *a* axis, which also acts to make α_b larger than α_a. Thus the greater stiffness along the *a* axis (the Young's moduli are equal to the inverses of the diagonal compliance moduli) inhibits thermal expansion along the *a* axis relative to that along the *b* axis.

The effects of the Poisson coupling of the transverse dimensions to the axial dimension are also considered, and the ratios of these off-diagonal complaince moduli are shown in Figure 6. For all of the calculations but one, this coupling is much larger in magnitude along the *a* axis, leading to decreased thermal expansion along the *a* axis relative to the *b* axis (it is not clear why the calculated results for the *Ibca* crystal with the KDG* force field differ so much from the other results; it was confirmed, however, that these results are not errone-

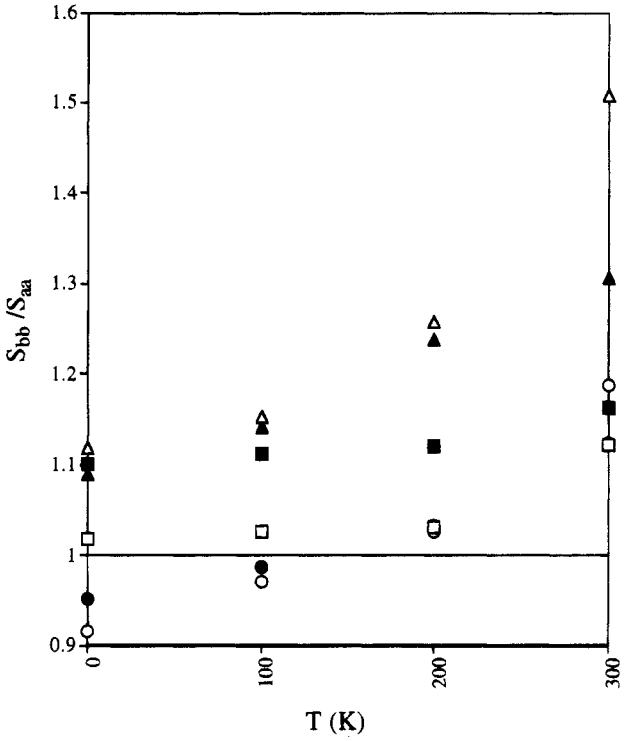

Figure 5. Ratio of the transverse compliance moduli for sPP. Symbols are the same as in Figure 3.

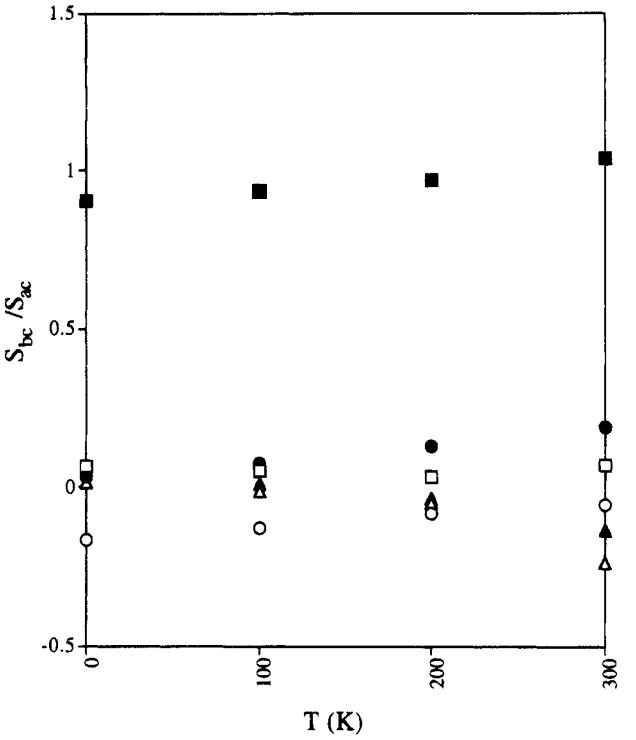

Figure 6. Ratio of the compliance moduli for coupling of the transverse directions to the axial direction for sPP. Symbols are the same as in Figure 3. This ratio is sometimes negative, because S_{bc} sometimes becomes slightly positive.

ous). The reason why the $a-c$ coupling is larger than the $b-c$ coupling is apparent from Figure 1, which shows that the sPP chain can be considered as a large zig-zag, with each segment of the zig-zag being an all-trans section of the chain. If the all-trans section is thought of as a moment arm, its projection along a is considerably greater than its projection along b, and thus an expansion or contraction of the zig-zag brought about by small variations in the soft intramolecular degrees of freedom (i.e., torsion angles, especially those in the higher energy gauche state) will lead to commensurately greater changes in the a dimension than in the b dimension.

The present calculations include the quantum mechanical effects in the vibrational motion. Although analagous classical calculations were not carried out, it is believed that the same qualitative results would be obtained even if the quantum effects were neglected, since our previous calculations on polyethylene showed that quantum effects influenced the transverse thermal expansion only slightly at room temperature.[2]

Conclusions

The thermal expansion of crystalline sPP is simulated. The approximate nature of the force fields limits any differentiation between the results for the different crystal structures, but the calculated results for the different structures and force fields bracket the experimental results of Lovinger *et al.* The calculated thermal expansion is greater along the b axis than along the a axis, in agreement with experimental results. This thermal expansion anisotropy is found to arise from larger thermal stresses, lower stiffness, and less Poisson coupling along the b axis.

References and Notes

(1) Lovinger, A. J.; Lotz, B.; Davis, D. D.; Schumacher, M. *Macromolecules* **1994**, *27*, 6603.
(2) Lacks, D. J.; Rutledge, G. C. *J. Phys. Chem.* **1994**, *98*, 1222.
(3) Lacks, D. J.; Rutledge, G. C. *Macromolecules* **1995**, *28*, 1115.
(4) Lacks, D. J.; Rutledge, G. C. *Chem. Eng. Sci.* **1994**, *49*, 2881.
(5) Lacks, D. J.; Rutledge, G. C. *Macromolecules* **1994**, *27*, 7197.
(6) Born, M.; Huang, K. *Dynamical Theory of Crystal Lattices*; Oxford University Press: Oxford, U.K., 1954. Venkataraman, G.; Feldkamp, L. A.; Sahni, V. C. *Dynamics of Perfect Crystals*; MIT Press: Cambridge, MA, 1975.
(7) Lacks, D. J.; Rutledge, G. C. *J. Chem. Phys.* **1994**, *101*, 9961.
(8) Sorensen, R. A.; Liau, W. B.; Kesner, L.; Boyd, R. H. *Macromolecules* **1988**, *21*, 200.
(9) Karasawa, N.; Dasgupta, S.; Goddard, W. A. *J. Phys. Chem.* **1991**, *95*, 2260.
(10) Natta, G.; Corradini, P.; Ganis, P. *J. Polym. Sci.* **1962**, *58*, 1191.
(11) Sozzani, P.; Galimberti, M.; Balbontin, G. *Makromol. Chem., Rapid Commun.* **1992**, *13*, 305.
(12) Corradini, P.; Natta, G.; Ganis, P; Temussi, P. A. *J. Polym. Sci., Part C* **1967**, *16*, 2477.
(13) Lotz, B.; Lovinger, A. J.; Cais, R. E. *Macromolecules* **1988**, *21*, 2375. Lovinger, A. J.; Lotz, B.; Davis, D. D. *Polymer* **1990**, *31*, 2253.
(14) DeRosa, C.; Corradini, P. *Macromolecules* **1993**, *26*, 5711.
(15) Sozzani, P. Simonutti, R.; Galimberti, M. *Macromolecules* **1993**, *26*, 5782.
(16) Lovinger, A. J.; Lotz, B.; Davis, D. D.; Padden, F. J. *Macromolecules* **1993**, *26*, 3494.

MA9505538